Diagn Interv Radiol 2022; 28:108–114

ABDOMINAL IMAGING

ORIGINAL ARTICLE

Arterial input function for quantitative dynamic contrast-enhanced MRI to diagnose prostate cancer

Farid Ziayee
Anja Mueller-Lutz
Janina Gross
Tim Ullrich
Michael Quentin
Christian Arsov
Gerald Antoch
Hans-Jörg Wittsack
Lars Schimmöller

PURPOSE
This study aims to analyze the ability of quantitative dynamic contrast-enhanced magnetic resonance imaging (DCE-MRI) to distinguish between prostate cancer (PCa) and benign lesions in transition zone (TZ) and peripheral zone (PZ) using different methods for arterial input function (AIF) determination. Study endpoints are identification of a standard AIF method and optimal quantitative perfusion parameters for PCa detection.

METHODS
DCE image data of 50 consecutive patients with PCa who underwent multiparametric MRI were analyzed retrospectively with three different methods of AIF acquisition. First, a region of interest was manually defined in an artery (AIF_m); second, an automated algorithm was used (AIF_a); and third, a population-based AIF (AIF_p) was applied. Values of quantitative parameters after Tofts (K^{trans}, v_e, *and* k_{ep}) in PCa, PZ, and TZ in the three different AIFs were analyzed.

RESULTS
K^{trans} and k_{ep} were significantly higher in PCa than in benign tissue independent from the AIF method. Whereas in PZ, K^{trans} and k_{ep} could differentiate PCa ($P < .001$), in TZ only k_{ep} using AIF_p demonstrated a significant difference ($P = .039$). The correlations of the perfusion parameters that resulted from AIF_m and AIF_a were higher than those that resulted from AIF_p, and the absolute values of K^{trans}, k_{ep}, and v_e were significantly lower when using AIF_p. The values of quantitative perfusion parameters for PCa were similar regardless of whether PCa was located in PZ or TZ.

CONCLUSION
K^{trans} and k_{ep} were able to differentiate PCa from benign PZ independent of the AIF method. AIF_a seems to be the most feasible method of AIF determination in clinical routine. For TZ, none of the quantitative perfusion parameters provided satisfying results.

Most malignant tumors, such as prostate cancers (PCa), demonstrate altered perfusion. Higher vascular permeability, neo-angiogenesis with greater microvessel density, and arteriovenous shunts represent the main reasons.[1] However, benign prostatic hyperplasia may also exhibit early perfusion and hinder accurate diagnosis of PCa especially in the transition zone (TZ) with magnetic resonance imaging (MRI) alone.[2] Dynamic contrast-enhanced MRI (DCE-MRI) shows differences of perfusion of a defined region of interest (ROI) in the examined tissue based on the change of signal intensity (SI). The repetitive image acquisition of the same slices requires a certain temporal resolution, so that in order to provide clinical feasibility, the chosen T1-weighted sequence usually represents a compromise between spatial and temporal resolution.[3] The SI changes over time can be converted into a concentration-time-curve (CTC), which provides information about the dynamics and distribution of contrast medium in the examined tissue.

The semi-quantitative analysis of DCE, integrated in the multiparametric protocol of PIRADS version 1 (together with T2- and diffusion-weighted imaging), has been exchanged for a qualitative and therefore, subjective analysis of DCE in version 2.[4] Quantitative DCE as in Tofts model[5] assumes two compartments in the examined tissue, representing extravascular extracellular space and blood plasma in an effort to provide absolute and therefore more objective values for perfusion.[3] In this model, the constants for the exchange rate of contrast medium between the two compartments (K^{trans} and k_{ep}) and the volume

From the Department of Diagnostic and Interventional Radiology (F.Z. A.M.L.✉ Anja.Lutz@med.uni-duesseldorf.de, J.G., T.U., M.Q., G.A., H.J.W., L.S.), and Department of Urology (C.A.), University Dusseldorf, Faculty of Medicine, Dusseldorf, Germany.

Received 3 February 2020; revision requested 19 March 2020; last revision received 19 December 2020; accepted 27 December 2020.

Published online 15 March 2022.

DOI: 10.5152/dir.2022.19512

You may cite this article as: Ziayee F, Mueller-Lutz A, Gross J, et al. Arterial input function for quantitative dynamic contrast-enhanced MRI to diagnose prostate cancer. *Diagn Interv Radiol*. 2022;28(2):108-114.

fraction of extracellular extravascular space within a voxel (v_e) are calculated. Although other methods have shown promising results,[6] the most common way to determine the perfusion parameters K^{trans}, k_{ep}, and v_e requires the determination of the arterial input function (AIF). Since the initial intravenous bolus of contrast medium becomes dispersed and delayed through the circulation, the AIF, which describes the time course of arterial contrast delivery to the tissue, is needed to interpret SI changes in the examined ROI. Thus, the AIF gives crucial information about tissue perfusion.

Objectivity and reproducibility of quantitative DCE analysis may ultimately endorse its routine use to optimize the detection of PCa in spite of the more complicated and time-consuming assessment. There are different methods for the acquisition of AIF. One common method suitable for clinical practice consists of drawing a ROI in a suitable artery such as the femoral artery manually. This manually acquired AIF requires further involvement of the radiologist. As an alternative, the AIF may be acquired by using automated algorithms, thus combining the advantage of a user independent and a patient specific AIF. Especially when a suitable artery is not available, the average of a population may serve as a solution. However, this population-based AIF is not specific to the examined patient. Since different methods for the determination of AIF, a standardized choice of method would be desirable for clinical and research purposes.[7]

The objective of this study was to compare values of quantitative perfusion parameters using Tofts two compartment model for PCa and physiologic tissue in TZ and peripheral zone (PZ) generated by three different methods of AIF determination.

Main points

- Automated AIF can be used as a standard user-independent time saving method.
- K^{trans} and k_{ep} can differentiate PCa from benign tissue in the peripheral prostate zone PZ.
- Quantitative DCE analysis was inferior for PCa detection in the TZ.

Methods

Study design

The study included 50 patients with prostate MRI and subsequently detected PCa (March 2013 to July 2014). The same consecutive patient collective with PCa was evaluated previously regarding the influence of AIF acquisition method on quantitative perfusion parameters and zonal prostate anatomy. Index lesions with biopsy proven PCa using targeted in-bore MRI-guided biopsy were included in the evaluation. All patients received additional systematic transrectal ultrasound-guided biopsy. This study was conducted in a university hospital setting and has been approved by the institutional ethical review board (protocol number of ethics committee approval: 3612). All patients provided written informed consent.

Study endpoints

The primary endpoint is to demonstrate a significant difference of quantitative perfusion parameters (K^{trans}, k_{ep}, and v_e) between PCa and benign prostatic tissue. Secondary endpoints focused on differences of performance between automated (AIF_a) and population-based (AIF_p) AIF in comparison to manual AIF (AIF_m) as a reference AIF.

Image acquisition, AIF determination, and quantitative perfusion parameter

The methods for image acquisition and for the determination of AIF_m, AIF_a, and AIF_p have been published before.[7,8] For AIF_m, a ROI was outlined in the common femoral artery. SI was converted into a CTC employing a linear approach by Mouridsen et al.[9] and multi-flip-angle approach.[10] For AIF_a, the same slice as in AIF_m was used. Cluster analysis with *k-means* function in MATLAB (MATLAB R R2011a, the Mathworks) was conducted. A ROI was created for AIF_a if the number of voxels in a cluster was between 10 and 80. The temporal resolution of our data was integrated in Parker's population-based AIF for AIF_p.[11]

Quantitative perfusion parameters after extended Tofts model (K^{trans}, v_e, and k_{ep}) were determined for each dataset in PZ-PCa and TZ-PCa as well as in physiological PZ and TZ tissues in the dynamic T1-vibe-sequence. K^{trans} and v_e, best fitting the CTC of each ROI, were determined using the MATLAB-function *fminsearch*.$_{ep}$ was then calculated as the quotient of K^{trans} and v_e.[5]

Statistical analysis

Statistical analysis was performed with MATLAB (MATLAB R R2011a, the Mathworks). Data were examined for normal distribution with the Kolmogorov-Smirnov test. Non-normally distributed data for independent samples were analyzed with non-parametric Mann-Whitney U test. Normally distributed data were tested with the Student t test. $P < .05$ was considered significant. Furthermore, receiver operating characteristic (ROC) analyses were conducted for every parameter of each AIF method. Performance was assessed by calculating the respective areas under the ROC curve (AUCs) and the maximum Youden index (J) with corresponding cutoff value, sensitivity, and specificity for each method and perfusion parameter. Correlations were determined with Spearman correlation coefficient with a value for correlation-coefficient ρ between 0.7 and 0.9 considered as strong and a value for ρ greater than 0.9 as very strong.[12] Descriptive statistics of the data are presented with n (%) and, for non-normalized variables, are shown as median (25-75 percentiles), and normally distributed data are shown as mean ± SD.

Results

Baseline characteristics with age, prostate-specific antigen (PSA), prostate volume, PSA density, and ISUP grade group separated by PCa localization (PZ or TZ) in the biopsied index lesions are shown in Table 1.

The absolute values of k_{ep} and K^{trans} in PCa were significantly higher for AIF_m, AIF_a, and AIF_p ($P < .001$), but not for v_e ($P = .898$ in AIF_m, $P = .837$ in AIF_a, and $P = .651$ in AIF_p). The Spearman correlation coefficient for the three different perfusion parameters K^{trans}, v_e, and k_{ep} between the different AIF methods AIF_m, AIF_a, and AIF_p are given in Table 2 with a $P < .001$ for each correlation. Spearman correlation coefficient was highest for k_{ep} ($\rho = 0.94$ for AIF_m-AIF_a, $\rho = 0.89$ for AIF_m-AIF_p, and $\rho = 0.86$ for AIF_a-AIF_p). Both AIF_m and AIF_a display a similar CTC with a peak of approximately 1 mmol/L, whereas in AIF_p, highest contrast medium concentration was 6 mmol/L.

Mean K^{trans}, v_e, and k_{ep} in PCa and in benign tissue with all three AIF methods is shown in Table 3 with their corresponding *P* values. The ROC curves reveal that k_{ep} has

Table 1. Baseline characteristics

	Patients	PCa in PZ	PCa in TZ	*P*
n (%)	50	37 (74)	13 (26)	
Age (years), mean ± SD	67 ± 7.1	67 ± 6.8	68 ± 8.5	.439*
PSA (ng/mL), median (IQR)	9.6 (7.1-14)	8.9 (6.6-13)	12.4 (20-43)	.071**
Prostate volume (mL), median (IQR)	46 (37-57)	46 (37-63)	46 (39-53)	.832**
PSA density (ng/mL/mL), median (IQR)	0.22 (0.15-0.34)	0.20 (0.13-0.33)	0.26 (0.19-0.43)	.104**
ISUP grade group, n (%)	1	7 (14)	2 (4)	
	2	16 (32)	8 (16)	
	3	7 (14)	1 (2)	
	4	4 (8)	1 (2)	
	5	3 (6)	1 (2)	

PZ, peripheral zone; TZ, transition zone; PCa, prostate cancer; ISUP, International Society of Urological Pathology.
*Student t test;
**Mann-Whitney U test.

Table 2. Correlation of quantitative perfusion parameters (K^{trans}, v_e, and k_{ep}) in PCa lesions between different AIF methods (AIF_m, AIF_a, and AIF_p)

	K^{trans}	v_e	k_{ep}	*P**
ρ (AIF_m-AIF_a)	0.87	0.74	0.94	<.001
ρ (AIF_m-AIF_p)	0.60	0.50	0.89	<.001
ρ (AIF_a-AIF_p)	0.61	0.53	0.86	<.001

ρ, Spearman rank correlation coefficient; AIF_m, manually acquired arterial input function; AIF_a, automated arterial input function; AIF_p, population-based AIF.
*P of Spearman correlation coefficient was <.001 for all correlation analyses.

a greater AUC in comparison to K^{trans} and v_e with the highest value in AIF_p (AUC_{max} = 0.859) (Figure 1a). Youden index was also generally greater for k_{ep} (J range: 0.52-0.61) in comparison to K^{trans} (J range: 0.4-0.48) and v_e (J range: 0.14-0.17) with the highest value in AIF_p (J_{max} = 0.61). Among the three methods, AIF_p demonstrates greater AUCs and Youden indexes in comparison to AIF_m and AIF_a for the parameters K^{trans} and k_{ep}.

Mean K^{trans}, v_e, and k_{ep} in PCa of PZ, PCa of TZ and in benign tissue in PZ or TZ with all three AIF methods are shown in Table 4. Differences between PCa in PZ and PCa in TZ were not statistically significant. When comparing PCa of PZ with benign tissue in PZ, K^{trans} and k_{ep} demonstrate significantly different values in all three methods. The ROC curves reveal for PCa in PZ that K^{trans} and k_{ep} have a greater AUC (AUC range: 0.849-0.890) and Youden indexes (J range: 0.55-0.68 for K^{trans}; J range: 0.58-0.68 for k_{ep}) in comparison with v_e (AUC range: 0.603-0.611) (J range: 0.26-0.32) (Figure 1b). K^{trans} in AIF_p has the highest AUC (AUC_{max} = 0.889) and Youden index (J_{max} = 0.68), followed by k_{ep} in AIF_p (AUC = 0.871, J = 0.67). For the differentiation of PCa in the TZ and benign TZ, *P* was only significant for k_{ep} in AIF_p with a $P < .001$, an AUC of 0.75, and a J of 0.50 (Figure 1c). Examples of colored K^{trans}, k_{ep}, and v_e maps of PCAs in TZ and PZ are shown in Figures 2 and 3.

Discussion

This study verified the ability of quantitative perfusion parameters K^{trans} and k_{ep} to distinguish PCa and benign prostate tissue in PZ, independent of the AIF method, while the performance in TZ was obviously inferior. This underlines a separate evaluation of each anatomical prostate zone.

Differences of absolute values of quantitative parameters gave rise to the question, in which AIF is best suited for PCa detection in clinical practice. The individualized nature of AIF_a and AIF_m, respecting patient's specific physiology, constitutes a major advantage over AIF_p. The similarities and the good correlation of results in AIF_a and AIF_m suggest that the cluster-based automated AIF generates acceptable results with the advantage of a user independent method. Other authors have identified K^{trans} and k_{ep} as best suited for differentiation of PZ and PCa.[13,14] Mehrabian et al.[15] also demonstrated that K^{trans} is capable to separate PCa and physiologic tissue in PZ, whereas v_e failed in PCa detection in the study by Ocak et al.[14] Bonekamp et al.[16] have shown that DCE contributes to a higher sensitivity and specificity of PCa detection in PZ. Our data demonstrate good results for K^{trans} and k_{ep} in all methods, while for TZ only k_{ep} resulting from AIF_p-processing was significant. There is a great variety for absolute

Table 3. Differentiation of PCa and benign tissue (PZ and TZ) by quantitative perfusion parameters (K^{trans}, v_e, and k_{ep}) in different AIF methods (AIF_m, AIF_a, and AIF_p)

		PCa	PZ and TZ	*P**
	K^{trans} (min^{-1})	0.64 (0.37-0.86)	0.32 (0.18-0.52)	
AIF_m	v_e	0.27 (0.21-0.33)	0.27 (0.18-0.35)	.898
	k_{ep} (min^{-1})	2.2 (1.58-3.32)	1.08 (0.84-1.57)	
	K^{trans} (min^{-1})	0.6 (0.38-0.84)	0.27 (0.17-0.47)	
AIF_a	v_e	0.21 (0.17-0.28)	0.22 (0.15-0.29)	.837
	k_{ep} (min^{-1})	2.49 (1.65-3.93)	1.26 (0.91-1.72)	
	K^{trans} (min^{-1})	0.11 (0.09-0.13)	0.07 (0.05-0.1)	
AIF_p	v_e	0.16 (0.14-0.18)	0.17 (0.13-0.2)	.651
	k_{ep} (min^{-1})	0.64 (0.57-0.88)	0.44 (0.31-0.51)	

Data are presented as median (Q1-Q3).
PZ, peripheral zone; TZ, transition zone; PCa, prostate cancer; AIF_m, manually acquired arterial input function; AIF_a, automated arterial input function; AIF_p, population-based AIF.
*Mann-Whitney U test.

Table 4. Differentiation of PCa and benign tissue regarding the localization by quantitative perfusion parameters and different AIF methods

		PCa in PZ	PZ	*P**	PCa in TZ	TZ	*P**	*P* (PCa in PZ vs. PCa in TZ)
AIF_m	K^{trans} (min^{-1})	0.65 (0.47-0.86)	0.26 (0.14-0.34)		0.46 (0.34-0.77)	0.42 (0.26-0.64)	.227	.338
	v_e	0.27 (0.21-0.32)	0.22 (0.15-0.31)	.101	0.28 (0.2-0.33)	0.32 (0.23-0.39)	.638	.927
	k_{ep} (min^{-1})	2.37 (1.76-3.32)	1.08 (0.84-1.57)		1.82 (1.45-2.67)	1.08 (0.84-1.57)	.071	.259
AIF_a	K^{trans} (min^{-1})	0.63 (0.38-0.85)	0.22 (0.14-0.36)		0.6 (0.35-0.75)	0.4 (0.24-0.58)	.232	.551
	v_e	0.21 (0.18-0.28)	0.19 (0.13-0.25)	.113	0.21 (0.15-0.28)	0.25 (0.19-0.32)	.820	.868
	k_{ep} (min^{-1})	0.72 (0.59-0.88)	1.26 (0.92-1.69)		1.88 (1.56-3.18)	1.26 (0.92-1.69)	.089	.401
AIF_p	K^{trans} (min^{-1})	0.11 (0.09-0.14)	0.05 (0.04-0.07)	<.001	0.1 (0.09-0.13)	0.09 (0.07-0.11)	.231	.590
	v_e	0.15 (0.14-0.18)	0.14 (0.1-0.19)	.122	0.17 (0.15-0.18)	0.18 (0.17-0.2)	.602	.158
	k_{ep} (min^{-1})	0.72 (0.59-0.88)	0.44 (0.31-0.51)		0.59 (0.5-0.7)	0.44 (0.31-0.51)		.162

Data are presented as median (Q1-Q3).
PZ, peripheral zone; TZ, transition zone; PCa, prostate cancer; AIF_m, manually acquired arterial input function; AIF_a, automated arterial input function; AIF_p, population-based AIF.
*Mann-Whitney U test.

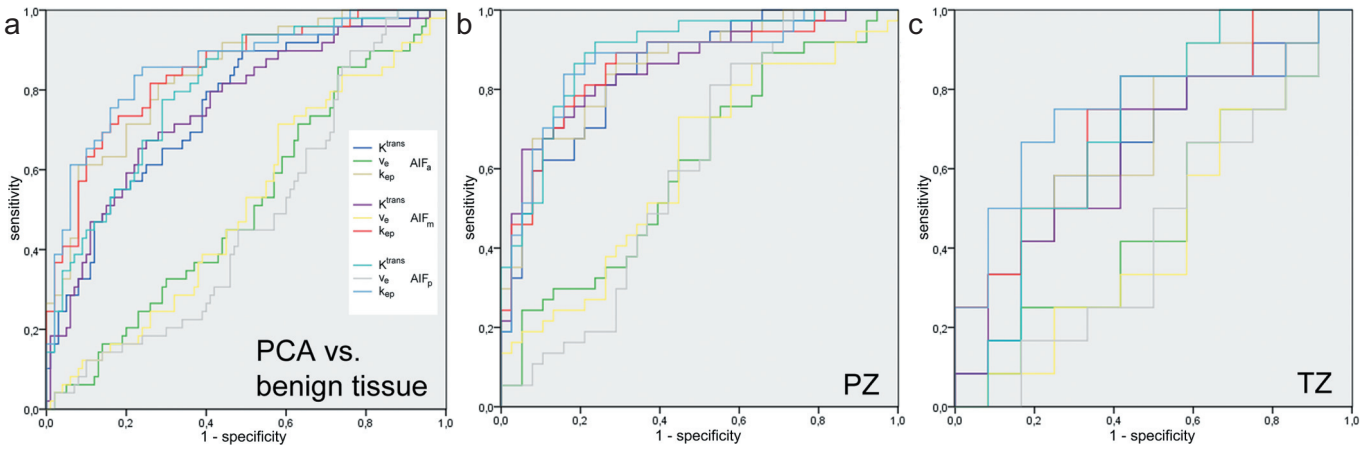

Figure 1. a-c. ROC analysis for quantitative perfusion parameters (K^{trans}, v_e, and k_{ep}) in different AIF methods (AIF_m, AIF_a, and AIF_p) for the distinction of PCa from benign tissue. Overall (PZ and TZ) **(a)**, in PZ **(b)**, and in TZ **(c)**.

values of K^{trans} between 0.16 (min^{-1})[13] and 0.61 ± 0.83 (min^{-1})[17] in AIF_p in physiologic PZ and 0.75 (min^{-1}).[13] and 186 ± 1.19 (min^{-1})[17] for PCa in current literature. Our K^{trans} values measured by AIF_a and AIF_m are within that range.[13,17] Our values for k_{ep} in all methods are within the range of results by Sanz-Raquena et al.[13] in physiologic tissue, but for PCa and using AIF_p, our results are lower. Individual patient's physiology affects the results in population-based AIF_p, as a major explanation for the different values and the relatively low correlation with AIF_m and AIF_a for perfusion parameters K^{trans} and v_e.[11] We noticed a very high peak in the CTC of AIF_p in comparison with AIF_m and AIF_a. It has been demonstrated by Meng et al.[17] that higher peaks result in smaller values for K^{trans}. Taking into account the relatively small sample size for TZ tumors and the deviating results for AIF_p (especially k_{ep}) in comparison with the reported values of other authors, the results may be caused by a sampling error. However, quantitative perfusion values resulting from AIF_m and AIF_a were in a realistic range, while the differentiation between PCa and PZ was equal to those measured by AIF_p. As AIF_a is user independent and resulted in nearly the same perfusion values as the AIF_m (as a standard method), this method seems to be most recommendable. The similar AUC values of K^{trans} and k_{ep} in PZ demonstrate that quantitative DCE analysis distinguishes PCa and benign tissue in PZ independently from the chosen AIF method. Brunelle et al.[18] found that the diagnostic performance of quantitative DCE parameters remains unchanged using different AIFs and MR imagers.

Absolute values of K^{trans} and k_{ep} of PCa in TZ and physiologic TZ tissue generally differed. Although this finding was statistically not significant, it might promote the consideration of DCE not only in PZ but also in TZ. Thus, positive enhancement might support selection of index lesions or in case of circumscribed enhancement in correlating encapsulated hyperplasia nodules can rule out PCa. A major reason for the difficulty of PCa detection by DCE in TZ is probably the higher vascularization of TZ hyperplasia in comparison to normal

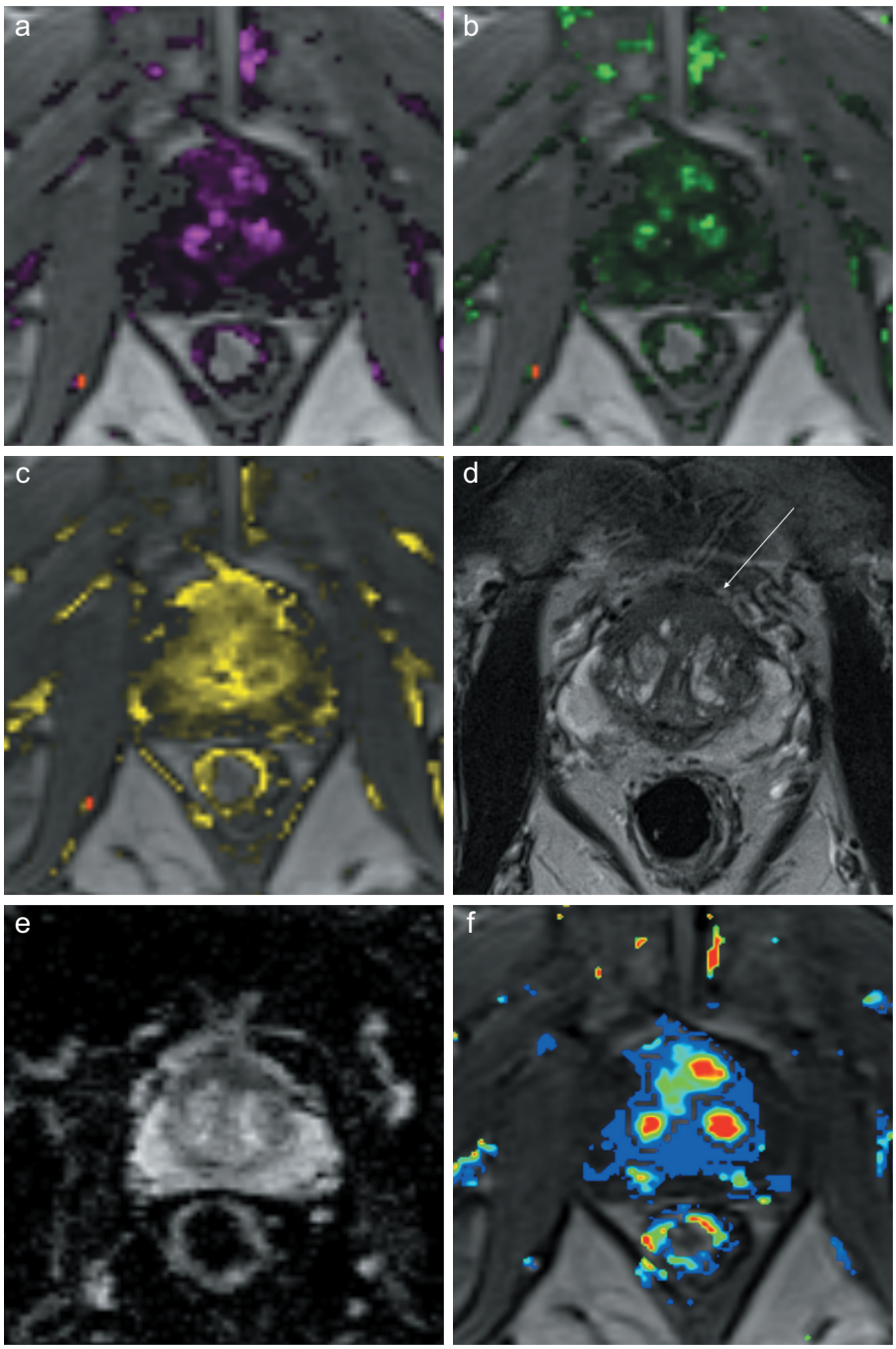

Figure 2. a-f. Axial images of PCa mid gland, anterior in TZ, and anterior fibromuscular stroma (*arrow* in T2 image, **d**). Colored maps of quantitative perfusion parameters K^{trans} (**a**, *purple*), k_{ep} (**b**, *green*), and v_e (**c**, *yellow*), T2-weighted images **(d)**, ADC map **(e)**, and DCE perfusion map (**f**, DynaCAD).

PZ tissue.[2] Also, current PI-RADS version (v2.1) supports qualitative DCE evaluation, since scientific evidence shows no clear benefit of quantitative DCE in PCa detection.[19] While some authors are completely against the standardized application of contrast medium due to similar performance in PCa detection of bi-parametric MRI (bpMRI) without DCE to prevent side effects, save costs and time,[20] a meta-analysis by Chen et al.[21] further supports DCE.[20,21] DCE seems be especially useful in PI-RADS 3 and 4 category lesions patients.[22] Therefore, PI-RADS v2.1 suggests that bpMRI is reserved for select clinical indications and multiparametric MRI with qualitative DCE analysis remains the standard approach.[19] However, quantitative analysis of DCE promises comparability and reproducibility of results and may improve sensitivity or specificity in PCa detection not only in PZ but also in TZ. Ullrich and Schimmöller[23] pointed out that lower inter-observer agreement caused i.a. =inter alia caused among others by the subjective nature of scoring criteria like used for qualitative DCE analysis. Future iterations of PI-RADS might include more quantitative analysis, if PCa detection can be improved compared to current purely qualitative assessment of DCE in version 2.1.

It has been shown previously that perfusion parameters differ significantly between benign PZ and TZ.[7] This does not seem to apply to PCa, since our study demonstrates similar characteristics of perfusion with no differences between PCa in PZ or in TZ.

Beyond the retrospective nature, this study has some limitations. Since there are numerous other methods for the acquisition of AIF, the chosen three methods in this study are exemplary, but not complete. The main question of whether quantitative evaluation after Tofts actually performs better than qualitative DCE evaluation, for example, as employed in version 2.1 of PIRADS analysis in PCa detection has not been investigated in this study since identification of index lesion was based on qualitative DCE analysis representing a potential bias. In addition, the advantage of additional DCE over a bi-parametric approach (with T2-weighted imaging and DWI) has not been explored. Validation of imaging findings is limited to MRI-guided biopsy and does not include surgical specimen. Also, added false positive lesions using quantitative DCE methods have not been analyzed. Furthermore, the sample size of TZ lesion subgroup was relatively small.

In conclusion, all AIF methods demonstrate satisfying results for the differentiation of PCa and PZ tissue. For absolute values and comparison between centers, an automated AIF that respects patient's individual physiology represents an attractive solution that does not require manual drawing of AIF by the radiologist. Quantitative DCE analysis seems inferior to identify PCa in TZ, but absolute

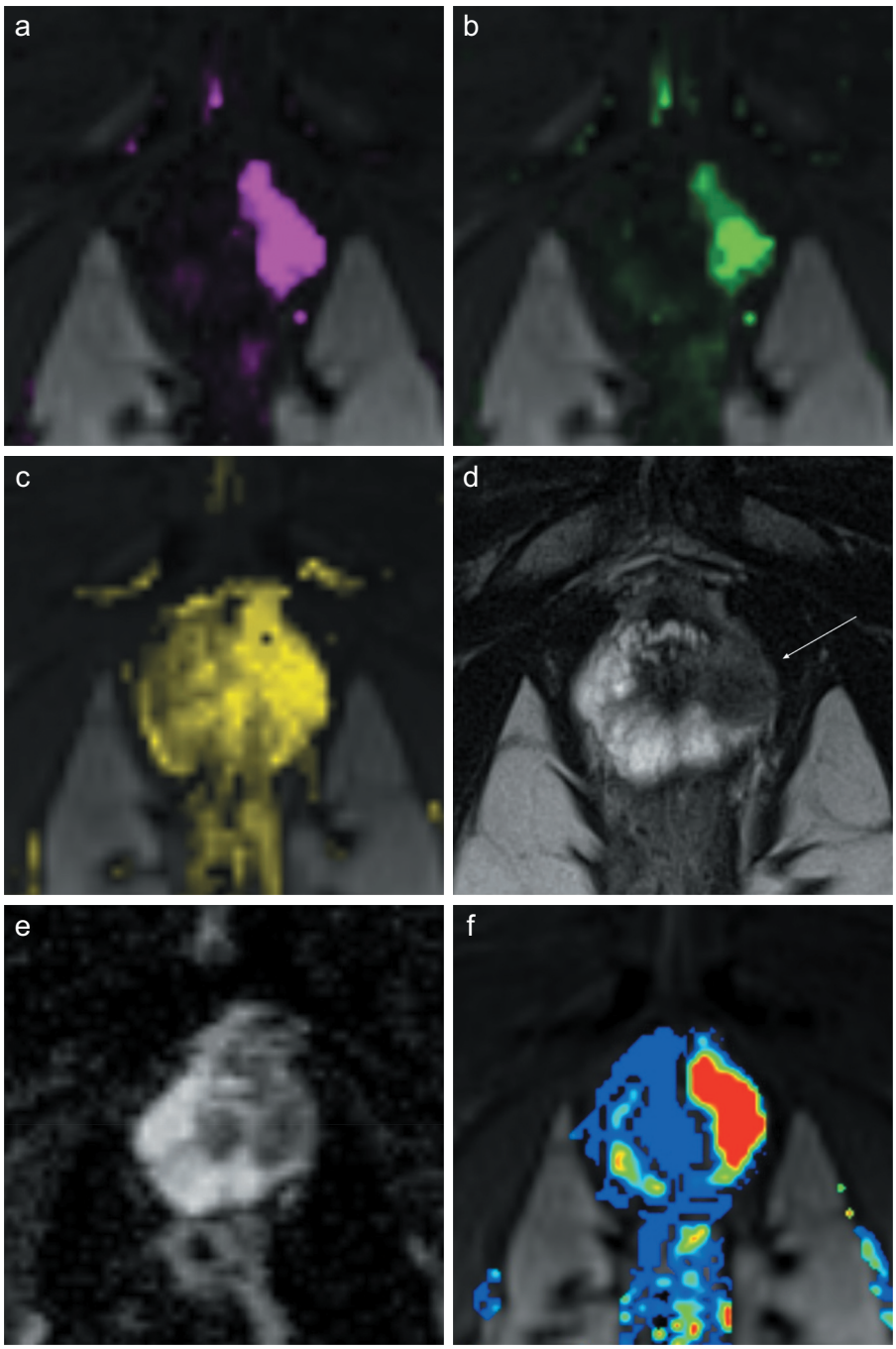

Figure 3. a-f. Axial images of PCa apical, posterolateral, and anterior on the left side in PZ (*arrow* in T2 image, **d**). Colored maps of quantitative perfusion parameters K^{trans} (**a**, *purple*), k_{ep} (**b**, *green*), and v_e (**c**, *yellow*), T2-weighted images **(d)**, ADC map **(e)**, and DCE perfusion map (**f**, DynaCAD).

results differed from physiologic tissue. This invites to consider DCE also for TZ lesions. The fact that all AIF methods allowed a differentiation of PCa and benign lesions and the good correlation for k_{ep} and K^{trans} may support quantitative analysis in clinical practice. The objective approach could facilitate the comparison between different centers in the future. Moreover, quantitative analysis with K^{trans} and k_{ep} could play an important role for therapy monitoring.

Conflict of interest disclosure

The authors declared no conflicts of interest.

References

1. Franiel T, Hamm B, Hricak H. Dynamic cont rast-enhanced magnetic resonance imaging and pharmacokinetic models in prostate cancer. *Eur Radiol*. 2011;21(3):616-626. [Crossref]
2. Ren J, Huan Y, Wang H, et al. Dynamic contrast-enhanced MRI of benign prostatic hyperplasia and prostatic carcinoma: Correlation with angiogenesis. *Clin Radiol*. 2008;63(2):153-159. [Crossref]
3. Tofts PS. T1-weighted DCE imaging concepts: Modelling, acquisition and analysis. *MAGNETOM Flash*. 2010;Supplement to RSNA Edition (3):30-39.
4. Rosenkrantz AB, Sabach A, Babb JS, et al. Prostate cancer: Comparison of dynamic contrast-enhanced MRI techniques for localization of peripheral zone tumor. *AJR Am J Roentgenol*. 2013;201(3):471-478. [Crossref]
5. Tofts PS, Brix G, Buckley DL, et al. Estimating kinetic parameters from dynamic contr ast-enhanced T(1)-weighted MRI of a diffusable tracer: Standardized quantities and symbols. *JMRI*. 1999;10(3):223-232. [Crossref]
6. Mischi M, Turco S, Lavini C, et al. Magnetic resonance dispersion imaging for localization of angiogenesis and cancer growth. *Invest Radiol*. 2014;49(8):561-569. [Crossref]
7. Ziayee F, Lueller-Lutz A, Gross J, Quentin M, Ulrich T et al. Influence of arterial input function (AIF) on quantitative prostate dynamic contrast-enhanced (DCE) MRI and zonal prostate anatomy. *Magn Reson Imaging*. 2018;53: 28-33. [Crossref]
8. Schimmöller L, Quentin M, Arsov C, et al. MR-sequences for prostate cancer diagnostics: Validation based on the PI-RADS scoring system and targeted MR-guided in-bore biopsy. *Eur Radiol*. 2014;24(10):2582-2589. [Crossref]
9. Mouridsen K, Christensen S, Gyldensted L, et al. Automatic selection of arterial input function using cluster analysis. *Magn Reson Med*. 2006;55(3):524-531. [Crossref]
10. Preibisch C, Deichmann R. T1 mapping using spoiled FLASH-EPI hybrid sequences and varying flip angles. *Magn Reson Med*. 2009;62 (1):240-246. [Crossref]
11. Parker GJM, Roberts C, Macdonald A, et al. Experimentally-derived functional form for a population-averaged high-temporal-resolution arterial input function for dynamic contrast-enhanced MRI. *Magn Reson Med*. 2006;56(5):993-1000. [Crossref]
12. Taylor R. Interpretation of the correlation coefficient: A basic review. *J Diagn Med Sonogr*. 1990;6:35-39. [Crossref]
13. Sanz-Requena R, Prats-Montalbán JM, Martí-Bonmatí L, et al. Automatic individual arterial input functions calculated from PCa outperform manual and population-averaged approaches for the pharmacokinetic modeling of DCE-MR images. *J Magn Reson Imaging*. 2015;42(2):477-487. [Crossref]
14. Ocak I, Bernardo M, Metzger G, et al. Dynamic contrast-enhanced MRI of prostate cancer at 3 T. A study of pharmacokinetic parameters. *AJR Am J Roentgenol*. 2007;189 (4):849. [Crossref]
15. Mehrabian H, Da Rosa M, Haider MA, et al. Pharmacokinetic analysis of prostate cancer using independent component analysis. *Magn Reson Imaging*. 2015;33(10):1236-1245. [Crossref]

16. Bonekamp D, Macura KH. dynamic cont rast-enhanced magnetic resonance imaging in the evaluation of the prostate. *Top Magn Reson Imaging*. 2008;19(6):273-284. [Crossref]
17. Meng R, Chang SD, Jones EC, et al. Comparison between population average and experimentally measured arterial input function in predicting biopsy results in prostate cancer. *Acad Radiol*. 2010;17(4):520-525. [Crossref]
18. Brunelle S, Zemmour C, Bratan F, et al. Variability induced by the MR imager in dynamic contrast-enhanced imaging of the prostate. *Diagn Interv Imaging*. 2018;99(4):255-264. [Crossref]
19. Turkbey B, Rosenkrantz AB, Haider MA, et al. Prostate imaging reporting and data system version 2.1: 2019 update of prostate imaging reporting and data system version 2.1. *Eur Urol*. 2019;76(3):340-351. [Crossref]
20. Van Der Leest M, Israel B, Cornel EB, et al. High diagnostic performance of short magnetic resonance imaging protocols for prostate cancer detection in biopsy-naïve men: The next step in magnetic resonance imaging accessibility. *Eur Urol*. 2019;2838 (19):30436-1 .[Crossref]
21. Chen Z, Zheng Y, Guanghai J, et al. Accuracy of dynamic contrast-enhanced magnetic resonance imaging in the diagnosis of prostate cancer: Systematic review and meta-analysis. *Oncotarget*. 2017;8(44):77975-77989. [Crossref]
22. Ullrich T, Quentin M, Arsov C, et al. Value of dynamic contrast-enhanced (DCE) MR imaging in peripheral lesions in PI-RADS-4 patients. *Röfo*. 2020;192(5):441-447.
23. Ullrich T, Schimmöller L Perspective: A critical assessment of PI-RADS 2.1. *Abdom Radiol (NY)* 2020; .[Crossref]